Fault Detection System Design and HILS Evaluation for the Smart UAV FCS

Yoonsu Nam, Huyeong Jang, Sung Kyung Hong, and Sungsu Park

Abstract: This paper is about a redundancy management system design for the Smart UAV (unmanned aerial vehicle) which utilizes the tilt-rotor mechanism. In order to meet the safety requirement on the PLOC (probability of loss of control) of 1.7×10^{-5} per flight hour for FCS (flight control system) failures, a digital FCS is mechanized with a dual redundant structure. A fault detection system which is composed of a CCM (cross channel monitor) and analytic redundancy using the Kalman filtering is designed, and its effectiveness is evaluated through experiments. A threshold level and persistence count for managing redundant sensors are designed based on the statistical analysis of the FCS sensors. To increase the survivability of the UAV after the loss of critical sensors in the SAS (stability augmentation system) and to provide reference information for a tie-breaking condition at which an ILM (in-line monitor) cannot distinguish the faulty channel between two operating ones, the Kalman filter approach is investigated.

Keywords: Cross channel monitor, fault detection, hardware in the loop simulation, Kalman filtering, stability augmentation system.

1. INTRODUCTION

Considering the failures due only to the flight control system (FCS), the probability of loss of control (PLOC) of a modern unmanned aircraft which uses a single channel FCS amounts to 2.0×10^{-4} per flight hour [1]. Considering the reliability of current technology for a one-channel operation, at least, duplex FCS redundancy is required to meet a stricter PLOC requirement than the above. Fault detection, isolation, and reconfiguration of redundant signals are very important processes in a real-time flight control system design called redundancy management (RM) [2,3]. An RM process can be divided into two sub-processes, i.e., monitoring and voting. Monitoring process is responsible for monitoring all redundant signals if any faults occur. A process of choosing a representative signal among redundant signals is called voting. An RM algorithm for a duplex FCS is depicted schematically in Fig. 1. All the processes described in the figure are executed every sampling time in the digital flight control computer. A process of analytic redundancy which replaces a function of sensor HW with some real-time executable codes by using a concept like a state estimator is shown in the dotted boxes. Through the application of analytic redundancy, the redundancy of the flight critical sensors such as rate gyros can be increased by a higher level, which results in the increase of the aircraft's safety.

To meet the PLOC requirement of 1.7×10^{-5} per flight hour, a duplex FBW/ FCS for the smart UAV was selected through a tradeoff study [4]. A cross channel monitor (CCM) is commonly used to determine the existence of any failures in the duplex redundant sensors. It is natural to conclude that a sensor channel out of the two-channels is in a faulty condition if a difference in-between gets consistently greater than a pre-calculated threshold (C_V) for more than a prescribed time (persistence count n). The existence of it in the duplex sensing system can be identified by using a CCM; however, it is impossible to discern the faulty channel between the two. An in-line monitoring (ILM) is the next step to apply in

Manuscript received June 28, 2006; accepted August 25, 2006. Recommended by Editorial Board member Hyo-Choong Bang under the direction of Editor Jae Weon Choi. This research was carried out for the Smart Unmanned Aerial Vehicles Development Program Center, one of the 21st Century Frontier R&D Programs funded by the Ministry of Science and Technology of Korea. It is also partly supported by the 2nd stage BK21 project.

Yoonsu Nam is with the School of Mechanical and Mechatronics Engineering, Kangwon National University, 192-2 Hyoja 2-dong, Chuncheon, Gangwon-do 200-701, Korea (e-mail: nys@kangwon.ac.kr).

Huyeong Jang is a graduate student in the Department of Mechatronics Engineering, Kangwon National University, 192-2 Hyoja 2-dong, Chuncheon, Gangwon-do 200-701, Korea (e-mail: jjakhead@hanmail.net).

Sung Kyung Hong and Sungsu Park are with the School of Mechanical and Aerospace Engineering, Sejong University, 98 Gunja-dong, Gwangjin-gu, Seoul 143-747, Korea (e-mails: {skhong, sungsu}@sejong.ac.kr).

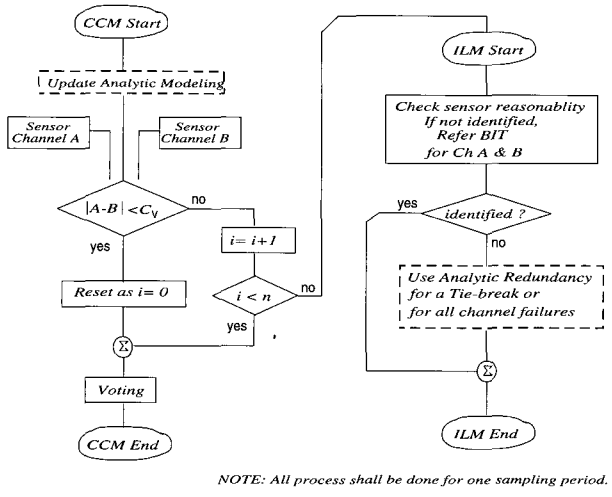

Fig. 1. RM algorithm in a digital processor.

order to determine the faulty channel. A reasonability check for the sensor signals, refering each sensor signal for any sensor output which is physically impossible to attain, or the BIT (built-in test) status checking is a common way of ILM. Analytic redundancy provides not only reference data for a tie-breaking condition, in which the application of ILM cannot distinguish the faulty one, but also the continuous flight critical information in a two-channel faulty condition. It means that some efforts can increase the survivability of the UAV even for a total loss in two rate gyros which are the critical components of the stability augmentation system (SAS).

This paper deals with the design methodologies for the CCM and analytic redundancy using the Kalman filtering. A discussion on the ILM design is omitted because its methodology is straightforward. The threshold level set-up C_V and persistence count n are covered in detail. Furthermore, analytic redundancy based on the Kalman filter is proposed. All the designs of CCM and analytic redundancy are verified through the hardware in the loop simulation(HISL). Two rate gyros *CRS03-02* from Silicon Sensing Systems [5] are installed on a one-axis motion table, which is real-time controlled by the digital processor *dSpace DS1103*. A flight dynamics of XV-15 at the hovering flight mode with a longitudinal SAS loop is considered as a baseline real-time dynamics.

2. CCM DESIGN METHODOLOGY AND EVALUATION

This section introduces a general CCM design methodology relying on the statistical analysis, after which some simulation results are presented for the verification.

2.1. CCM design methodology

The CCM design starts with the safety requirement on the air vehicle's PLOC due to the failures in the FCS. The PLOC of the Smart UAV is targeted for less than 1.7×10^{-5} per flight hour. In order to meet the requirement for a duplex FCS, the CCM coverage for the probability of the CCM to function successfully should be greater than 0.99 for a given channel failure rate of 2.0×10^{-4} per flight hour for each channel [4]. In general, most of the sensor output signals have a Gaussian distribution centered at its mean value. Therefore, the difference in the two sensor outputs can substantially deviate from the value of zero. If we set the threshold value of the CCM to be excessively low, a high chance of false alarm can be generated, which means the CCM recognizes a normal operating condition as a fault. The false alarm rate is a function of the threshold value (C_V) and persistence count (n). Therefore, designing a CCM coverage greater than 0.99 is absolutely equivalent to appropriately set C_V and n for the false alarm rate to be less than 0.01.

Assume that a noise component in the sensor has a Gaussian distribution with the standard deviation of σ_i. It follows that the difference signal between two sensor channels implies a Gaussian distribution with the standard deviation of $\sqrt{2}\sigma_i(\triangleq\sigma)$ [6]. The following assumptions are essential for a further discussion:

(1) A noise signal in the sensor has a normal distribution of $N(0,\sigma_i)$.
(2) The total flight hour for the Smart UAV is 5.
(3) The UAV dynamics is digitally controlled by a digital processor with the sampling rate of 50Hz.

When the threshold value, C_V, is set to $\pm\sigma\bar{C}_V$ as shown in Fig. 2(A), the probability of the deviation of the channel difference value from $\pm\sigma\bar{C}_V$ is $2F(-\sigma\bar{C}_V)$, where $F(\bullet)$ represents the cumulative

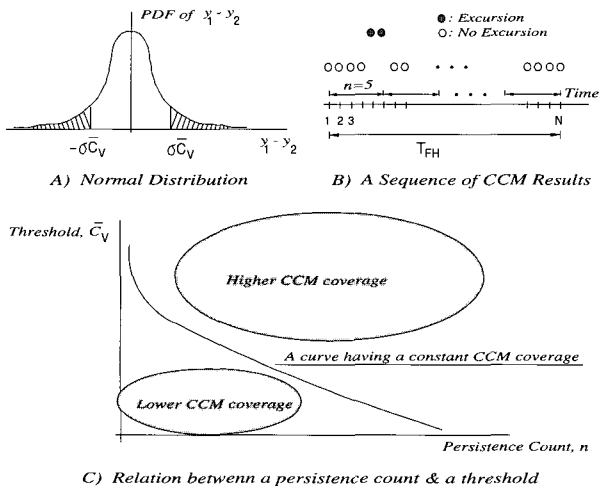

Fig. 2. Design concept of a CCM.

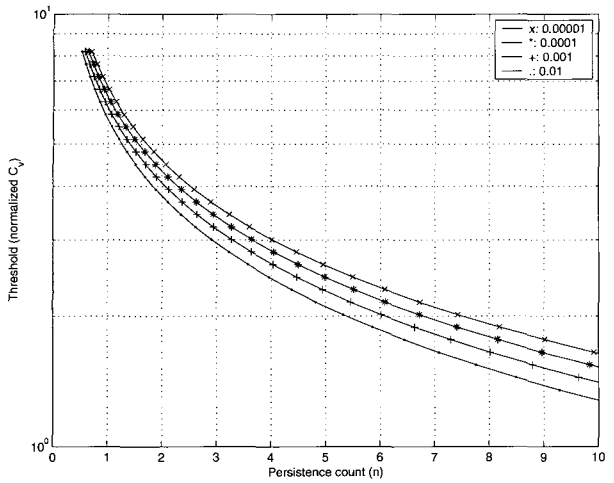

Fig. 3. Threshold and persistence count.

density function of a random process with a Gaussian distribution. As illustrated in Fig. 1 and Fig. 2(B), the RM modules are executed every sampling time for a total of N (= total flight hour÷sampling time) times. If the channel difference gets greater than $\pm\sigma\bar{C}_V$ and further continuously than n times, the CCM interprets this condition as a fault: The CCM wrongly judges one of the two channels as a fault. In order to control the false alarm rate to be less than 0.01 for the total flight hours, the threshold ($\sigma\bar{C}_V$) and persistence count (n) should be set to satisfy the following inequality.

$$\frac{\mathrm{N}\times(2F(-\sigma\bar{C}_V))^n}{n} \le 1 - CCM\,coverage \qquad (1)$$

As conceptually demonstrated in Fig. 2(C), the left term in (1) reduces towards a value of less than 0.01 for a greater $\bar{C}_V$ or n [7]. The CCM, however, becomes less sensitive to the drift or offset type sensor error. As the persistence count (n) increases, the presence of an unremoved faulty channel can jeopardize the vehicle dynamics. Therefore, a proper setting of the two CCM design parameters, the threshold ($\sigma\bar{C}_V$) and persistence count (n), is a crucial process. Fig. 3 is another way of presentation for (1). The four lines characterize the relations of n with $\bar{C}_V$ for the false alarm rate when the values of the left term of (1) are 0.01, 0.001, 0.0001, and 0.00001. A dotted line corresponds to the case of a false alarm rate of 0.01. It can be straightforward to set n and $\bar{C}_V$ if this figure is used. To ensure the CCM coverage of 0.99 for n=5, the threshold, $\bar{C}_V$, should be set at greater than 2.11. The CCM design procedure described in this section can be applied to any FCS sensor system.

2.2. CCM design evaluation

The CCM design described above is evaluated with the XV-15 tilt rotor flight dynamics. The linearized longitudinal XV-15 dynamics at the hovering mode is presented in (2). The units for linear and angular displacement are *ft*, and *radian*. δ_{LN} is the cyclic pitch displacement with the unit *inch* [8].

$$\begin{Bmatrix}\dot{u}\\ \dot{w}\\ \dot{q}\\ \dot{\theta}\end{Bmatrix}=\begin{bmatrix}0 & 0.003 & -0.037 & -32.15\\ -0.027 & -0.203 & 0.999 & -1.18\\ 0.0014 & 0 & -0.429 & 0\\ 0 & 0 & 1 & 0\end{bmatrix}\begin{Bmatrix}u\\ w\\ q\\ \theta\end{Bmatrix}+\begin{pmatrix}1.21\\ -0.022\\ -0.277\\ 0\end{pmatrix}\delta_{LN}$$

$$\begin{Bmatrix}q\\ \theta\\ V_A\end{Bmatrix}=\begin{bmatrix}0 & 0 & 1 & 0\\ 0 & 0 & 0 & 1\\ 0.9993 & 0.0367 & 0 & 0\end{bmatrix}\begin{Bmatrix}u\\ w\\ q\\ \theta\end{Bmatrix} \qquad (2)$$

As shown in Fig. 4, the SAS loop of XV-15 consists of two feedback sensors (q and θ) and PI controller. The noise effects of the sensors are included, and the average of the duplex redundant signals is used as a feedback signal for the two-channel operation.

Table 1 summarizes the characteristics of a CRS03-02 rate gyro [5] used as a pitch rate gyro for the SAS loop in Fig. 4. The uncertainty level can be drawn as follows.

$$V_{OUT} = k\cdot\Omega + V_0, \qquad (3)$$

where V_{OUT} : rate gyro output (volts),

k : sensitivity of a rate gyro (volts/ (deg/s))

$$k = f(\mathrm{V}_S,T) \cong k_0 + \left.\frac{\partial k}{\partial \mathrm{V}_S}\right|_0 \Delta\mathrm{V}_S + \left.\frac{\partial k}{\partial T}\right|_0 \Delta T$$

$$= 2\times10^{-2} \pm 8\times10^{-4} + 4\times10^{-3}\Delta\mathrm{V}_S,$$

Ω : angular rate (deg/s),

V_S : supply voltage (volts),

T : operating temperature (^oC),

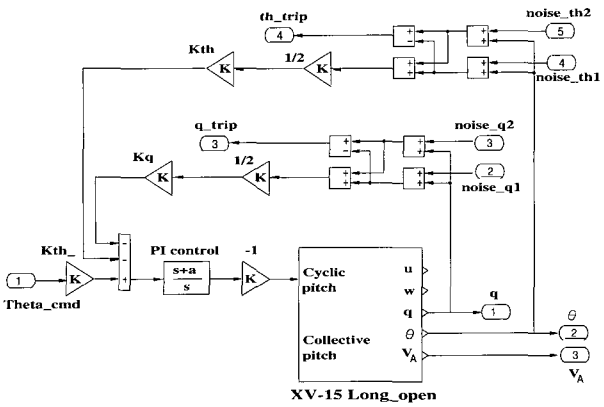

Fig. 4. SAS loop of XV-15 with sensor noises.

Table 1. Specification of a CRS03-02 rate gyro.

characteristics	unit	value
rate range	/s	$0 \sim \pm 100$
sensitivity	mV/(/s)	20
initial sensitivity error	%	± 1
sensitivity over temp^{+}	%	± 3
nonlinearity	% of full scale	0.5
bias	% of V_S	50
bias initial error	mV	± 60
bias over temperature	mV	± 60
quiescent noise	mV_{RMS}	1

$^{+}$: $-40 \sim 85^{o}C$

V_0 : output bias (volts)

$$V_0 = g(V_S, T) + n \cong 2.5 \pm 6 \times 10^{-2} + \left.\frac{\partial V_0}{\partial V_S}\right|_0 \Delta V_S + \left.\frac{\partial V_0}{\partial T}\right|_0 \Delta T + n \cong 2.5 \pm 0.12 + 0.5\Delta V_S + n,$$

n: quiescent noise (mV).

The variation of the sensor output signal from its nominal value is given as:

$$\Delta V_{OUT} = V_{OUT} - (V_{OUT})_{nom} = \pm 8 \times 10^{-4}\Omega + (4 \times 10^{-4}\Omega + 0.5)\Delta V_S + n. \quad (4)$$

If we assume the following operating conditions for a normal flight of the Smart UAV, the standard deviation of the CRS03-02 rate gyro can be calculated by using (5) [9].

(1) The peak pitch rate is less than 20deg/s.
(2) The standard deviation of the supply voltage (V_S) is less than 0.025.
(3) The standard deviation of the pitch rate response during the hovering flight is less than 2deg/s.

$$(\sigma)_{\Delta V_{OUT}} = \sqrt{\left(8 \times 10^{-4}\right)^2 \sigma_\Omega^2 + 0.58^2 \sigma_{\Delta V_S}^2 + \sigma_n^2} = 0.0146\ volts = 0.7311\ deg/s \quad (5)$$

The HILS (hardware in-loop simulation) setup prepared for a CCM design evaluation is schematically shown in Fig. 5. Not only the XV-15 flight dynamics but also a SAS loop and CCM logic for the pitch rate and angle signal can be executed in real-time by the digital processor *dSpace DS1103*. The pitch rate (q) and angle (θ) calculated in real-time are used as commanding signals for a motion table (Acutronic BD125). A CRS03-02 rate gyro installed on the motion table can pick up a pitch rate of XV-15 dynamics. The CRS03-02 output and rotational angle of the motion table are sampled in dSpcae DS1103 and used as feedback signals and CCM logic. Prior to

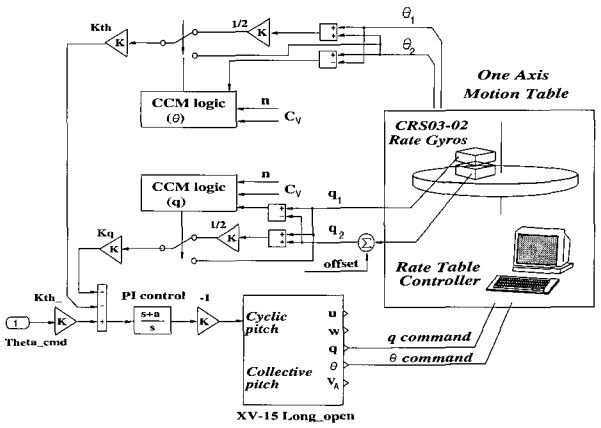

Fig. 5. HILS setup for the CCM design evaluation.

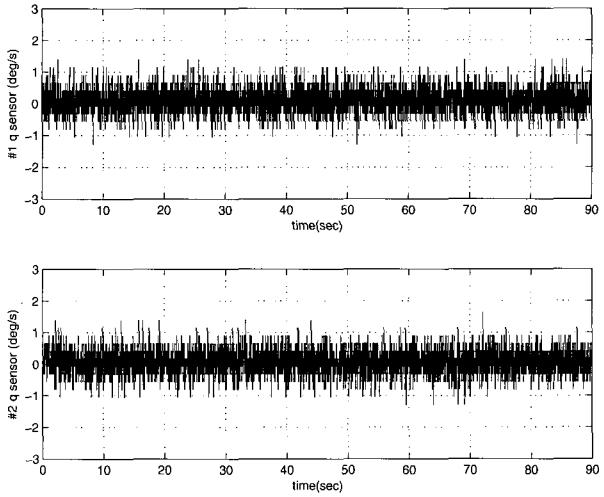

Fig. 6. Output signals from two CRS03-02 gyros at a static condition.

the hardware in the loop simulation, the assumption for an uncertainty amount of CRS03-02 represented by (5) was evaluated. The two sensor output signals are monitored for 90 seconds at a static condition, as shown in Fig. 6. The experimental standard deviation of the sensor output in this condition is approximately 0.3914deg/s, concluding that the uncertainty assumption by (5) is reasonable.

The experimental results for HILS summarized in Fig. 7 shows the response of the pitch angle, two pitch rates (q_1 & q_2), and trip counts for q and θ signals. For the zero commanding on q and θ, an intentional offset of -1, -2, -3, -4, and +2deg/s was added to the q_2 sensor output from 10 seconds during the HILS simulation. The following CCM logic was applied:

(1) Persistence count, n=5 and threshold, $\bar{C}_V$ =2.11.
(2) A fault channel, q_2, is always isolated by an ILM and removed from the SAS loop after n=5.
(3) The average of the two channel signals is used as a feedback signal for the SAS loop in a normal condition. Based on (2), a good channel like q_1 is

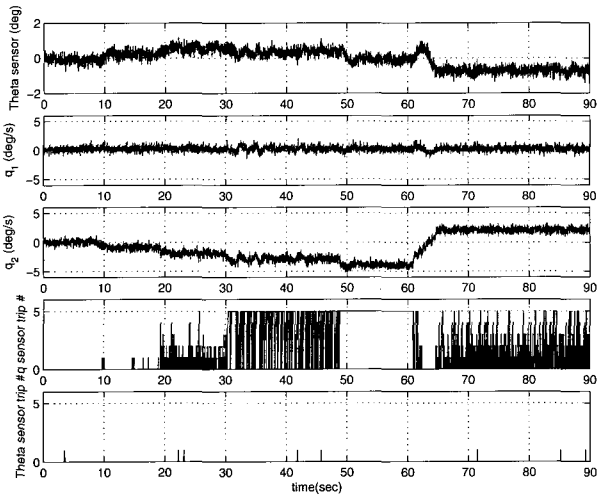

Fig. 7. HILS results for a CCM design evaluation.

selected for a one-channel operation.

(4) The trip count is reset as soon as the channel difference is within the threshold value.

Because of the zero position commanding for the motion table, the output signals of the q and θ sensors should be zero. However, these signals fluctuate due to the offset fault in the q_2 sensor. As noted in the former study [11], the offset-type fault in a q-sensor has a direct effect on the θ-response, but no effect on the q-response in a DC frequency range. The effect of yet eliminated offset fault in the q_2 signal is clearly shown in the first plot in Fig. 7 (θ sensor signal). The reason that the effect of the offset fault on the θ-response decreases for a greater magnitude offset (from 30 to 60 seconds in the HILS simulation) arises from the CCM logic (3) and (4) aforementioned. A magnitude offset fault of ±2deg/s in a q_2-sensor (from 20 to 30 seconds and from 64 to 90 seconds in the HILS simulation) is not eliminated by the CCM, but degrades the performance of the SAS loop. For a offset fault of 3deg/s (from 30 to 50 seconds in the HILS simulation), a continuous switching of the CCM logic takes place between two-channel (averaged q feedback) and one-channel operations (healthy q_1 feedback). The XV-15 dynamics for an offset fault of 4deg/s (from 50 to 60 seconds in the HILS simulation) follows the zero commanding again, because a faulty channel always remove the SAS loop.

3. ANALYTIC REDUNDANCY USING THE KALMAN FILTERING

Analytic redundancy technique can be applied to generating a reference signal to the tie-breaking condition, or to maintaining a flight dynamics kept in control even in a critical condition like the total loss of q-sensor information in the SAS loop. This section introduces a concept of designing analytic redundancy using the Kalman filtering. For a discrete dynamic

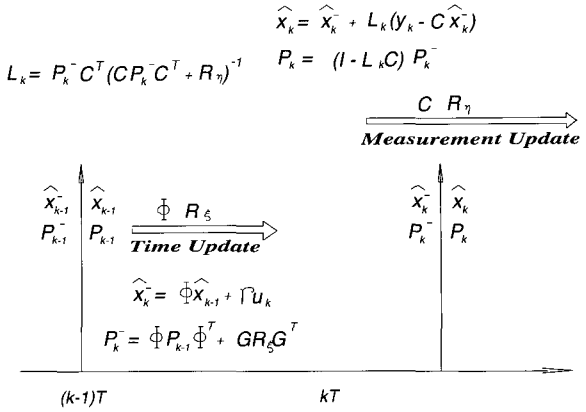

Fig. 8. A structure of a discrete Kalman filter.

system of (6), the Kalman filter is composed of two steps: time update and measurement update [10], as described in Fig. 8.

$$\begin{aligned} x_k &= \Phi x_{k-1} + \Gamma u_k + G\xi_k \\ y_k &= Cx_k + \eta_k \end{aligned} \tag{6}$$

Time update:

$$\begin{aligned} \hat{x}_k^- &= \Phi \hat{x}_{k-1} + \Gamma u_k, \\ P_k^- &= E\left\{(x_k - \hat{x}_k^-)(x_k - \hat{x}_k^-)^T\right\} \\ &= \Phi P_k^- \Phi^T + G R_\xi G^T. \end{aligned} \tag{7}$$

Measurement update:

$$\begin{aligned} \hat{x}_k &= \hat{x}_k^- + L_k(y_k - C\hat{x}_k^-), \\ L_k &= P_k^- C^T (C P_k^- C^T + R_\eta)^{-1}, \\ P_k &= E\left\{(x_k - \hat{x}_k)(x_k - \hat{x}_k)^T\right\} = (I - L_k C) P_k^-. \end{aligned} \tag{8}$$

When all the two-channel sensor data are healthy or ILM works properly to isolate a one-fault channel, there is no need to use the results of the Kalman filtering. Equations (7) and (8) are updated in the digital flight control computer every sampling time. In case two-channels are in a faulty condition or ILM does not work, analytic redundancy can supply the time-critical data to the flight control system of the Smart UAV as follows:

(1) Update state estimation using the time update equation in (7).

(2) Recalculate the Kalman filter gain, L_k, based on a new output matrix C and R_η which excludes the row corresponding to a faulty sensor, and performs the measurement update equation in (8).

(3) An analytic sensor signal can be reconstructed by multiplying the row deleted in the previous step (2) with the measurement updated state estimate.

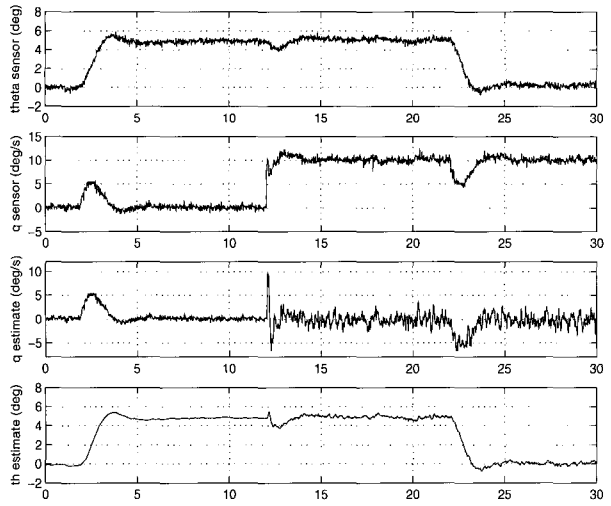

Fig. 9. HILS results for the evaluation of a discrete Kalman filter.

Fig. 9 shows the HILS results obtained by using the same experimental setup as for Fig. 5. The scenario for this simulation is as follows: Two pitch rate gyros have been working in a good condition up to 12 seconds. However, it is assumed that one channel out of the two has an offset error of 10deg/s, which is not isolated by ILM. Therefore, the flight critical software has to rely on the analytic redundancy to find the faulty channel. However, the offset fault causes a direct impact on the XV-15 flight dynamics, at least, for the period of 0.1 second (i.e., n×sampling time= 5×0.02). The effects of this fault channel can be noticed as some glitches in responses of Fig. 9 at around 12 seconds. The first and fourth plots are the pitch angle sensor output and its estimate, and the second and third ones are the pitch rate sensor output and its estimate. Fig. 9 shows that the analytic redundancy technique based on the Kalman filtering is properly working, which means the estimates from the Kalman filtering, i.e., the results of an analytic redundancy, can provide a good reference signal for a tie-breaking condition or flight critical information for the SAS loop of the XV-15. Notice further that the magnitude of the noise component in the estimation signals gradually increases after the application of analytic redundancy.

4. CONCLUSION

An RM (redundancy management) design methodology for a duplex redundant flight control system is introduced. Two parameters in the CCM design, i.e., threshold and persistence count, are selected based on the statistical analysis. Analytic redundancy using the Kalman filtering is also proposed. The validity of the design methodologies is checked by the hardware in the loop simulation, where the *CRS03-02* rate gyro is installed on the motion table to pick up a pitch rate of XV-15 dynamics solved in real-time by the digital processor *dSpace DS1103*. It turns out that the proposed analytic redundancy based on the Kalman filtering properly works, meaning that the estimates from the Kalman filtering, i.e., the results of an analytic redundancy, can provide a good reference signal for a tie-breaking condition or flight critical information for the SAS loop of the Smart UAV.

REFERENCES

[1] S. O. Ku, "System engineering in the smart UAV technology development (A)," *The 2nd Progress Review Workshop on the Smart UAV*, 2004.

[2] S. Osder, "DC-9-80 digital flight guidance system monitoring techniques," *Journal of Guidance and Control*, vol. 4, no. 1, pp. 41-49, 1981.

[3] K. W. Vieten, J. D. Snyder, and R. P. Clark, "Redundancy management concepts for advanced actuation systems," *Proc. of AIAA/AHS/ASEE Aerospace Design Conference*, AIAA 93-1168, Irvine, CA, pp. 1-9, 1993.

[4] Y. Nam, S. K. Hong, and C. S. Yoo, "A study on the FCS redundancy level for the smart UAV," *Proc. of Conference for the Korean Society of Aerospace and Aeronautical Engineers*, pp. 412-415, April 2003.

[5] http:// www.spp.co.jp/sssj/silicon-e.html

[6] R. Walpole and R. Myers, *Probability and Statistics for Engineers and Scientists*, MacMillian Publishing Company, 1985.

[7] "Sensor redundant management: The development of a design methodology for determining threshold values through a statistical analysis of sensor output data," *NASA-CR-173270*, 1983.

[8] L. G. Hofmann, R. H. Hoh, W. F. Jewell, G. L. Teper, and P. D. Patel, "Development of automatic and manual flight director landing systems for the XV-15 tilt rotor aircraft in helicopter mode," *NASA TR No. 1092-1*, 1978.

[9] E. O. Doebelin, *Measurement Systems Application and Design*, 4th edition, Chapter 3, McGraw-Hill Publishing Company, 1990.

[10] A. Gelb, *Applied Optimal Estimation*, Chapter 4, The MIT Press, 1979.

[11] Y. Nam, S. K. Hong, and C. S. Yoo, "Redundancy management for a duplex FBW flight control system," *Journal of the Korean Society of Aerospace and Aeronautical Engineers* (Korean), vol. 32, no. 10, pp. 46-52, 2004.